On the question of two-step nucleation in protein crystallization[†]

Andrea Sauter[a]**, Felix Roosen-Runge**[b]**, Fajun Zhang**[*a]**, Gudrun Lotze**[c]**, Artem Feoktystov**[d]**, Robert M. J. Jacobs**[e]**, and Frank Schreiber**[a]

1 Supporting Information

The electrophoretic mobility was used to determine the zeta potential of proteins as a function of the salt concentration. By this method, charge inversion was verified. The measurements were done using a Zetasizer Nano ZS from Malvern Instruments Ltd with a 633 nm laser. Although the reentrant effect for BLG solutions in the presence of $CdCl_2$ is not complete, a charge inversion with increasing divalent salt concentration is observed, see Fig. S1. Compared to previous work[1], the charge inversion of BLG is weaker and occurs at higher salt concentrations than with the trivalent salt YCl_3[1,2]. The phase boundaries are shifted towards higher salt concentrations, too. This relative weak charge inversion may explain the phase behavior observed, i.e. a $pseudo - c**$ or a transition zone and the sample solutions in the third regime are still a bit turbid.
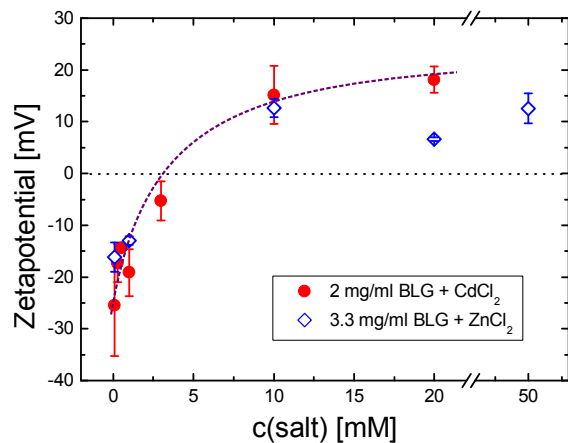
Fig. S1 Zeta potential measurements on 2 mg/ml BLG with increasing $CdCl_2$ concentrations. The dotted red line is a guide to the eye, the dashed black line marks a charge of 0.

Protein crystallization followed by real-time SAXS measurements. Samples contain 33 mg/ml BLG with 15 - 20 mM $CdCl_2$ in the transition zone of *pseudo-c***. Fig. S2 shows additional SAXS data for 33 mg/ml BLG with 15 and 18.5 mM $CdCl_2$.
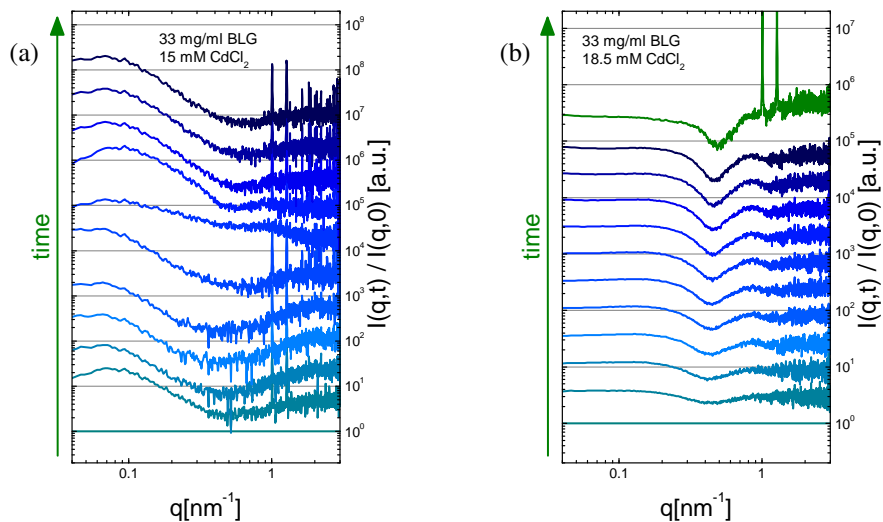

Fig. S2 Real-time SAXS curves for 15 mM $CdCl_2$ (a) and 18.5 mM (b).

Fig. S3 shows the kinetic evolution for a two-step process as modeled by rate equations with parameters reproducing the experimental findings from Figure 8b in the main manuscript.
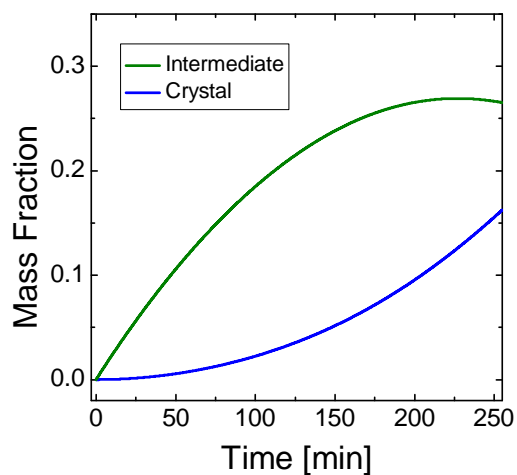
Fig. S3 Kinetic evolution for a two-step process as modeled by rate equations. The following parameter values were used to show the good qualitative agreement of the model with the data set: $k_e = 0.15\,\text{min}^{-1}$, $L_0 = 0.2$, $\alpha_I = 0.2$, $k_{gL} = 0.6\,\text{min}^{-1}$ (same as for Figure 9c in the main manuscript), $k_I = 0.003\,\text{min}^{-1}$, $k_n = 0.002\,\text{min}^{-1}$, $k_{gI} = 0.02\,\text{min}^{-1}$.

The number of crystals in solutions with 33 mg/ml BLG and different $CdCl_2$ concentrations around $pseudo - c^{**}$ observed by microscopy can also be followed in the videos listed in the following:

- The first video shows the crystallization in presence of 17 mM $CdCl_2$ (file of the same title is attached). The crystals are numerous and small.

- The second one shows the crystallization in presence of 20 mM $CdCl_2$ (file of the same title is attached). Compared to the previous video, significantly fewer and larger crystals can be observed.

Another animation provided with this publication shows the fitting performed for evaluation of the amount of MIP and crystalline phase for a sample with 17 mM $CdCl_2$: "SAXSdecomposition.gif". Link to animation. Both the broad peak and the Bragg peaks have been fitted by scaled Gaussians and their enclosed areas evaluated.

References

1 F. Zhang, G. Zocher, A. Sauter, T. Stehle and F. Schreiber, *J. Appl. Cryst.*, 2011, **44**, 755–762.
2 A. Sauter, M. Oelker, G. Zocher, F. Zhang, T. Stehle and F. Schreiber, *Crystal Growth and Design*, 2014, **14**, 6357–6366.